On the Nature of Unrestricted Orbitals in Variational Active Space Wave Functions

Gregory J. Beran*

Department of Chemical Engineering, Massachusetts Institute of Technology, Cambridge, Massachusetts 02139

Martin Head-Gordon

Department of Chemistry, University of California and Chemical Sciences Division, Lawrence Berkeley National Laboratory, Berkeley, California 94720-1460

Received: March 23, 2006; In Final Form: June 9, 2006

Active space coupled cluster methods exhibit unusual, nonsmooth spin symmetry-breaking behavior where the unrestricted minimum lies higher in energy at short bond distances and crosses below the restricted solution at longer distances. The restricted solution is also observed to be a stable minimum slightly beyond the symmetry-breaking point. This behavior arises due to differences in the optimal active spaces defining the restricted and unrestricted wave functions and results in unrestricted wave functions that are not strictly size consistent. We suggest a new, size-consistent model that allows the orbitals to break spin symmetry only within the active space.

Introduction

In writing down the equations for unrestricted Hartree−Fock (UHF) theory in 1954, Pople and Nesbet recognized that, "There is no a priori reason, however, why any of the orbitals in one [spin] set should be identical with any in the other."[1] In the limit of the exact wave function, full configuration interaction (FCI), there is no advantage to any particular representation of the alpha and beta spatial orbitals—all give the same FCI energy. Approximate wave functions, on the other hand, can sometimes benefit variationally from breaking spin or spatial symmetry. In the former, the alpha and beta spatial orbitals differ, whereas in the latter, the molecular orbitals no longer transform according to the point-group symmetry of the molecule. In this article, we only consider spin symmetry breaking (SB).

Symmetry breaking in quantum chemistry is a tradeoff—the variationally lower energy of the symmetry-broken solution is often desirable, but the solution often lacks desirable properties inherent to the exact wave function. For example, unlike their restricted counterparts, unrestricted wave functions are not eigenfunctions of the spin operator $\hat{S}^2$. The rapid changes in the wave function for small geometric shifts near the SB point leads to deformed potential energy surfaces and spurious property predictions, such as the infamous cases where perturbation-theory-predicted harmonic vibrational frequencies are hundreds or even thousands of wavenumbers in error.[2−4] Furthermore, Møller−Plesset perturbation series based on highly spin-contaminated UHF solutions exhibit extremely poor convergence with respect to higher-order terms in the perturbative expansion.[5−7] On the other hand, restricted wave functions typically overbind species significantly, and are not size-consistent. Deciding whether to grant the wave function the flexibility to break symmetry depends in large part on the problem at hand and the researcher's goals.

Spin SB becomes variationally advantageous when the approximate wave function lacks the flexibility to properly describe the system. For example, restricted Hartree−Fock (RHF) theory cannot properly describe homolytic bond dissociation to give an electron localized on each fragment.[8] Instead, in the RHF long-bond-length limit, both electrons share a spatial orbital spread over both fragments. Spin symmetry breaking allows the alpha bonding orbital to localize to one fragment and the beta bonding orbital to localize to the other, leading to the qualitatively correct dissociation limit (at the expense of the wave function no longer being an eigenfunction of $\hat{S}^2$). Because of their often better energetics, unrestricted methods are routinely used for treating open-shell systems, bond dissociation, transition states, diradicals, and other systems with highly correlated electronic structure.

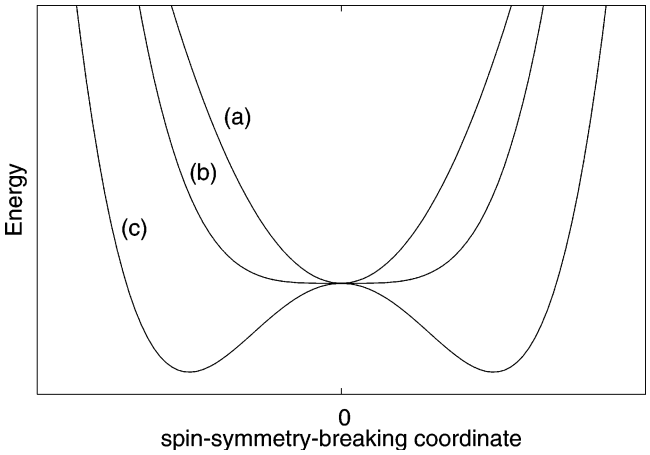

Figure 1. Schematic of a typical orbital rotation energy surface with respect to breaking spin symmetry in the orbitals (a) before the SB point, (b) at the SB point, and (c) after the SB point.

To understand the orbital behavior near the SB point, consider the wave function near equilibrium along a bond-breaking coordinate on the potential energy surface (PES). In this region, the RHF (or related method) solution is a minimum with respect to orbital rotations along the spin symmetry-breaking coordinate, as shown schematically in Figure 1, curve a. However, at some

* Corresponding author. E-mail: gberan@mit.edu.

10.1021/jp061814q CCC: $33.50
Published on Web 07/27/2006

point during the stretch, the second derivative of the energy with respect to SB orbital rotations becomes zero (curve b), allowing the wave function to change significantly with no change in the energy. Beyond the SB point (curve c), the unrestricted solution becomes variationally preferred, and the restricted solution lies at a saddle point between two equivalent unrestricted solutions in the orbital rotation space.

Given the limitations of HF in providing a qualitatively correct reference determinant for highly correlated systems such as radicals, diradicals, and transition states, research efforts have focused on simplified correlated wave functions that include a description of the static correlation effects that are so important in these systems. Perhaps the most ubiquitous of these approaches is the so-called complete active space self-consistent field (CASSCF) wave function,[9] in which the FCI problem is solved within a small subset of active orbitals, the number of which typically corresponds to the chemically interesting orbitals. The partitioning between active and inactive orbitals is determined variationally. Because they provide the exact solution within the active space, CASSCF wave functions are invariant to mixing between active occupied and active virtual orbitals. Instead, the energy depends only on the partitioning between three subspaces: inactive occupied orbitals, active orbitals (both occupied and virtual), and inactive virtual orbitals. Unfortunately, the factorial scaling of CASSCF with respect to the size of the active space size limits its applicability to systems with up to about 14 active orbitals and electrons.

Active space coupled cluster methods, such as valence orbital-optimized coupled cluster doubles (VOD),[10] and an unrestricted coupled cluster formulation of perfect pairing (PP)[11−15] have been developed as less expensive approximations to CASSCF for the treatment of systems exhibiting strong static correlation effects. Instead of solving the FCI problem, VOD solves the coupled cluster doubles (CCD)[16] equations in an active subset of the orbitals. As in CASSCF, the actual orbitals are obtained by variationally minimizing the active space CCD energy with respect to orbital rotations. In contrast to HF, for which the energy depends solely on the partitioning between the occupied and virtual subspaces, or CASSCF, for which the dependence is described above, the VOD energy depends on the partitioning between four subspaces: the uncorrelated core occupied, the active occupied, the active virtual, and the uncorrelated inactive virtual orbital subspaces.

PP can be viewed as a strongly local approximation to VOD that pairs the active electrons and allows only one correlating orbital per electron pair.[17,18] The simplicity and computational affordability of PP makes it a promising candidate to replace HF in many classes of systems for which static correlation is important.[14,18] The local approximation inherent in PP destroys the invariance between active occupied or active virtual orbitals found in VOD. Instead, PP is generally only invariant toward mixing between inactive occupied or inactive virtual orbitals (a more complete discussion of the invariances found in PP has been presented previously[19]). All of these active space methods can provide accurate energetics for many challenging systems when coupled with perturbative corrections (e.g., CASPT2,[20] VOD(2),[21] or PP(2)[19]) to account for the remaining dynamical electron−electron correlations.

Because these methods variationally optimize the molecular orbitals based on a correlated wave function that provides a better reference description of the system, they tend to be more resistant to spin SB.[22] In fact, because it solves the FCI problem in the active space, CASSCF would be expected to exhibit distinct unrestricted solutions only if the chosen active space were too small to describe the important correlations in the system under study. Because VOD and PP describe active space correlations more approximately, they break spin symmetry more frequently, albeit often at longer bond distances than does HF.[14,22]

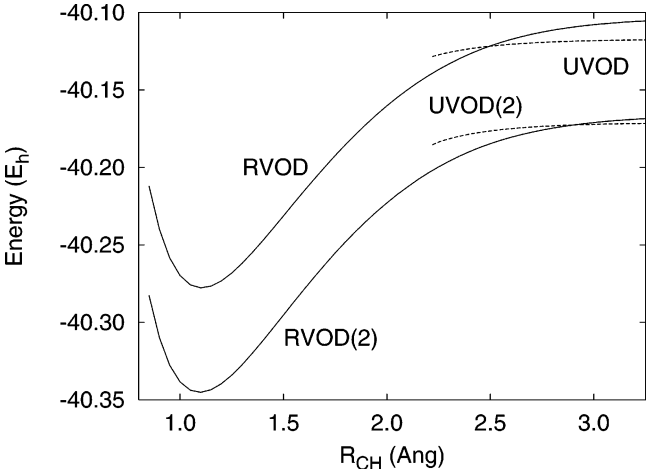

Figure 2. Restricted and unrestricted hydrogen abstraction from CH_4 with VOD and VOD(2) in the 6-31G* basis, using the perfect pairing active space.

However, as was recently noted, these active space methods exhibit an unusual feature[19] not found in HF and other full-space methods: they break spin symmetry nonsmoothly, exhibiting a discontinuity in the first derivative of the energy with respect to nuclear displacement. Because the exact PES must be both smooth and continuous, such discontinuities and kinks are indicative of an ill-defined Ansatz. For example, local correlation methods of the style pioneered by Saebø and Pulay[23] define the terms contributing to the correlation energy based on spatial criteria, leading to discontinuities in regions of the PES where interorbital distances cross the cutoff threshold.[24] Because of the obvious problems this creates for studying potential energy surfaces, an important criterion for a model chemistry is that it should produce smooth, differentiable surfaces with changes in nuclear geometry.[17] Like the aforementioned local models, UVOD and UPP fail this test, but for a completely different reason, as we shall see.

In fact, as we will demonstrate, this UVOD and UPP SB behavior is quite general and can occur with any active space method that does not solve FCI within the active space. Here we explain the origin of this odd SB behavior in terms of orbital subspace partitionings and discuss its implications for size consistency. The results we find lead logically to a new model in which the space spanned by the alpha and beta core orbitals, active orbitals (the union of both active occupied and active virtual), and inactive virtual orbitals are constrained to be identical. Spin symmetry breaking is allowed only within the active space.

Spin Symmetry Breaking in Variational Active Space Methods

Figure 2 plots the restricted and unrestricted VOD and VOD(2) solutions in the 6-31G* basis[25] for abstracting a hydrogen atom from methane with all other atoms fixed ($R_{CH} = 1.10$ Å, $\angle HCH = 109.5°$). The active space consists of four σ_{CH} bonding orbitals and four σ^*_{CH} antibonding orbitals of each spin type. These PESs were obtained from energies computed every 0.05 Å from 0.85 to 3.25 Å and every 0.01 Å near curve intersections. All calculations were performed using a developmental version

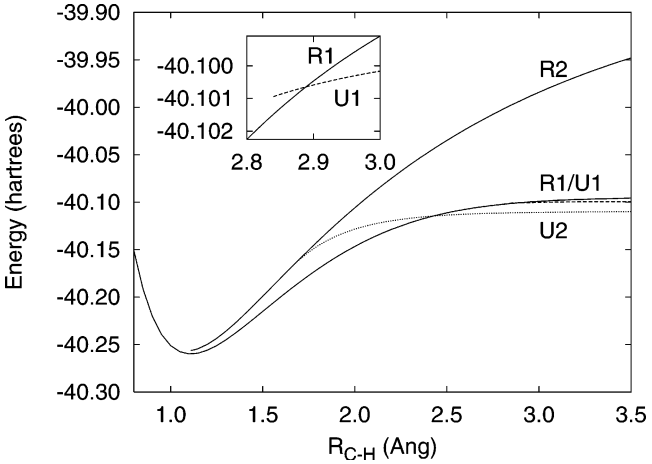

Figure 3. Various restricted (solid) and unrestricted (dashed) solutions for hydrogen abstraction from CH_4 with PP/cc-pCVDZ. (Inset) *R*1/*U*1 SB region.

of Q-Chem.[26] The use of methane as the species is representative—similar PESs have been observed for numerous other species. We were only able to converge the unrestricted VOD solution as short as 2.22 Å. Below that, the solution tends toward the lower-energy restricted one.

Looking at Figure 2, we observe a nonsmooth (discontinuous first derivative of the energy with respect to nuclear displacement) restricted to unrestricted transition between 2.49 and 2.50 Å for VOD. In contrast, orbital optimized coupled cluster doubles (OD),[27] which is equivalent to VOD with all orbitals active, exhibits standard SB behavior with the restricted and unrestricted solutions coinciding before the SB point.

This nonsmooth SB effect is potentially more severe when the VOD wave function is corrected perturbatively. If the perturbative correction is defined as the correction from the variationally lowest VOD reference solution, we would observe a sizable energy discontinuity in the VOD(2) energy near 2.5 Å, where UVOD becomes lower in energy. If one instead chooses to follow the lowest of the two VOD(2) solutions along the PES, VOD(2) exhibits a continuous but nonsmooth restricted to unrestricted transition at 2.9 Å, where UVOD(2) becomes lower in energy.

Results similar to VOD were found for PP in the cc-pCVDZ/RI-cc-pVDZ basis set,[28,29] as shown in Figure 3, where a nonsmooth crossover between solutions labeled *R*1 and *U*1 occurs at 2.89 Å. Furthermore, we were able to locate an alternate set of restricted and unrestricted solutions, denoted *R*2 and *U*2, respectively, that are characterized by an unusual active space consisting of correlations for the three unstretched C−H bonding pairs and for the C 1s pair. The bond-breaking pair is inactive. In contrast to the solutions found for VOD and to *R*1/*U*1, these solutions break symmetry smoothly, like HF, at 1.67 Å. For comparison, HF/cc-pCVDZ breaks symmetry at 1.66 Å.

Though it lies high in energy near equilibrium, at dissociation, solution *U*2 is variationally preferred over the more chemically sensible solution *U*1, and it makes an earlier SB point at 2.43 Å. Presumably, one could also locate other, higher-energy solutions corresponding to the replacement of unstretched C−H bonding pairs with the C 1s pair in the active space, though we did not search for them.

Stability analysis (computed by finite difference of the analytical gradients) at the PP level indicates that both solutions *R*1 and *U*1 are minima (all eigenvalues of the orbital Hessian are positive) in the orbital rotation space before, at, and for a short distance after the *R*1/*U*1 crossover point, as shown in Table 1. *R*1 does not become unstable (with one negative Hessian eigenvalue) until 2.92 Å, 0.03 Å after the SB point, in marked contrast with the SB behavior of HF! As expected, following this instability leads to solution *U*1. Neither *R*1 nor *U*2 exhibits any instabilities in the region of their crossover (i.e., near 2.43 Å). On the other hand, solution *U*2 branches smoothly from *R*2 when *R*2 becomes unstable at its SB point (1.66 Å), behaving exactly like HF would. For all points beyond the *R*2/*U*2 SB point, *R*2 is unstable and *U*2 is stable, and for all points before the SB point, the two solutions coincide.

TABLE 1: Smallest Eigenvalues of the Orbital Rotation Hessian for PP near the Various SB Points for CH_4 Hydrogen Abstraction

R (Å)	*R*1	*U*1	*R*2	*U*2
1.66			0.000251[d]	0.000251[d]
1.67[a]			−0.003482	0.002484
1.68			−0.007293	0.002481
2.42	0.004222			0.002476
2.43[b]	0.003988			0.002476
2.86	0.000077	0.001578		
2.89[c]	0.000029	0.001385		
2.90	0.000015	0.001298		
2.91	0.000003	0.001212		
2.92	−0.000009	0.001131		
2.95	−0.000037	0.000916		

[a] *R*2/*U*2 SB point [b] *R*1/*U*2 SB point [c] *R*1/*U*1 SB point [d] *U*2 and *R*2 coincide.

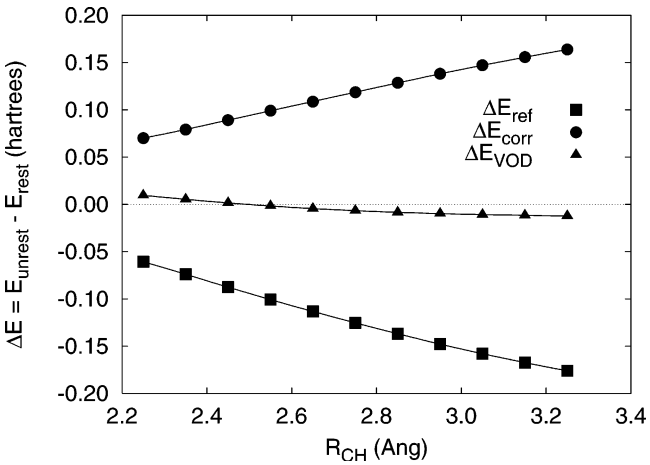

Figure 4. $\Delta E = E_{\text{unrest}} - E_{\text{rest}}$ for the reference energy, the correlation energy, and the total energy for methane dissociation at the VOD/6-31G* level.

To understand the behavior, we examine the VOD solutions in more detail. Spin SB can be viewed as an energetic competition between the restricted and unrestricted correlated wave functions. In the absence of correlation, the single-determinantal reference (e.g., HF/6-31G*) would break spin symmetry at 1.65 Å, when the unrestricted single determinant becomes energetically favored. However, spin SB decreases the magnitude of the correlation energy of the system (defined here as $E_{\text{corr}} = E_{\text{VOD}} - E_{\text{ref}}$), because the unrestricted correlations are more atomic in nature. Plots of the difference $\Delta E = E_{\text{unrest}} - E_{\text{rest}}$ for the single-determinant reference, the correlation energy, and the VOD energy are presented in Figure 4. As the bond is stretched, the unrestricted reference becomes much more stable than the restricted one, making ΔE_{ref} very negative. Conversely, the correlation energy is much stronger (more negative) for the restricted wave function, making ΔE_{corr}

TABLE 2: Smallest Orbital Overlap Values between Restricted and Unrestricted VOD Orbital Subspaces Slightly before (R_{CH} = 2.45 Å) the SB Point[a]

	$\langle R\|U^{\alpha}\rangle$	$\langle R\|U^{\beta}\rangle$
core	1.00	1.00
act. occ.	0.82	0.81
act. vir	0.77	0.37
inact. vir.	0.93	0.45

[a] All other overlaps not listed are >0.99.

positive. The competition between these two effects delays the SB point (where ΔE_{VOD} becomes negative) until 2.5 Å, after which the UVOD solution is favored. This argument also applies to other correlation methods where the orbitals are reoptimized (OD, for example) and explains their increased stability against SB, but it does not explain the coexistence of separate restricted and unrestricted solutions before the SB point.

Next, we examine the two wave functions near the crossover point. Because the VOD wave function and energy are defined by the space spanned by the four orbital subspaces (core, active occupied, active virtual, and inactive virtual), we compare the partitioning between these spaces in the restricted and unrestricted wave functions at a given geometry. The molecular orbital coefficients defining the VOD wave function are denoted as:

$$C^{R} = [C^{R}_{core} C^{R}_{act.occ.} C^{R}_{act.vir.} C^{R}_{inact.vir.}] \quad (1)$$

for the restricted case, and

$$C^{U\alpha} = [C^{U\alpha}_{core} C^{U\alpha}_{act.occ.} C^{U\alpha}_{act.vir.} C^{U\alpha}_{inact.vir.}] \quad (2)$$

and

$$C^{U\beta} = [C^{U\beta}_{core} C^{U\beta}_{act.occ.} C^{U\beta}_{act.vir.} C^{U\beta}_{inact.vir.}] \quad (3)$$

for the unrestricted case.

To understand how they differ, we compute the corresponding orbitals[30] separately for each of the four subspaces between the restricted orbitals and the alpha and beta unrestricted orbitals. These orbitals are formed by computing the eight molecular orbital overlap matrices $\mathbf{D} = \langle R|U^{spin}\rangle$ between the two solutions for each of the four subspaces, including:

$$\mathbf{D}^{RU\alpha}_{core} = \langle R_{core}|U^{\alpha}_{core}\rangle = C^{R}_{core}{}^{\dagger} S_{AO} C^{U\alpha}_{core} \quad (4)$$

and

$$\mathbf{D}^{RU\beta}_{core} = \langle R_{core}|U^{\beta}_{core}\rangle = C^{R}_{core}{}^{\dagger} S_{AO} C^{U\beta}_{core} \quad (5)$$

and so on, where S_{AO} represents the atomic orbital overlap matrix. These matrices are diagonalized using the singular value decomposition, and the molecular orbitals transformed to the new basis. Note that the transformed restricted orbitals, $\tilde{C}^{R}$, differ depending on whether the overlap with the alpha or beta unrestricted orbitals was diagonalized.

Upon performing this analysis on the VOD solutions at R_{CH} = 2.45 Å, each subspace contained at most one overlap less than 0.99. The smallest overlap for each subspace is listed in Table 2. This bond length was chosen because it lies shortly before the SB point, though the results obtained vary little throughout the region. The restricted and unrestricted solutions have virtually identical core subspaces, as indicated by the essentially perfect overlap. Their alpha active occupied, beta active occupied, alpha active virtual, and alpha inactive virtual subspaces differ moderately, whereas their beta active and inactive virtual subspaces differ significantly.

The corresponding orbitals for the least-overlapping orbitals obtained from this procedure are plotted in Figure 5 using Molden,[31] enabling us to compare how the wave functions differ. The unrestricted wave function is, to a good approximation, obtained by exchanging each plotted restricted orbital with its unrestricted counterpart.

For both wave functions, the core orbitals are simply the C 1s orbitals and are relatively uninteresting. The active occupied orbital of interest changes from a C−H σ-bonding orbital (restricted) to a H 1s (alpha unrestricted) and a C sp-hybrid (beta unrestricted). This shift is the standard spin SB behavior one would expect. The alpha active virtual switches from a C−H σ*-antibonding orbital (restricted) to a C sp-hybrid (unrestricted), and the alpha inactive virtual shifts density slightly toward the hydrogen. In the beta virtual space, the H 1s counterpart to the unrestricted active virtual is moved to the inactive virtual space. In its place, a formerly inactive virtual with significant C sp-character is made active. These changes in the virtual subspaces maximize the correlation energy by increasing the fraction of the active space lying on the carbon atom, which has a greater potential for correlation interactions than does the hydrogen atom.

Elsewhere, we have observed the exchange of the unrestricted "bonding" active occupied orbital and a core orbital,[14] in this case pushing the H 1s orbital into the core space, and making the C 1s active. When the H 1s orbital is far enough away, it becomes almost totally uncorrelated with the other electrons. In that event, even the weak correlations involving the C 1s orbital are stronger than those with the H 1s orbital, so the variationally determined active space will reflect this.

By expanding the active space on one fragment at the expense of another, the unrestricted wave function changes and does not approach the proper dissociation limits, meaning that it is not size consistent. Instead, the singlet state CH_3−H supersystem at a 50 Å separation lies 9.9 millihartrees (6.2 kcal/mol) lower than the sum of the individual doublet state fragment energies with UVOD, as shown in Table 3. This lack of strict size consistency arises directly from the unconstrained orbital optimization in the unrestricted methods, and it occurs despite the fact that VOD, as a coupled cluster method, is manifestly extensive with molecular size.

The PP solutions presented earlier exhibit similar features to the VOD ones. Solution *U*1 arises primarily from a mixing between the active and inactive virtual orbitals analogous to that observed for UVOD. *U*2, on the other hand, has the spin SB occurring solely in the inactive core space (where the dissociating pair resides). Therefore, the active space does not change between *R*2 and *U*2 at the SB point, and it breaks spin symmetry smoothly. This RHF-like treatment of the bond-breaking pair also explains why the SB point occurs essentially at the same distance as for HF and why the asymptote of *R*2 is so high in energy. At long distance, the correlation energy of the unrestricted bonding pair is smaller in magnitude than the correlation energy for the C 1s pair, so *U*2 lies lower than *U*1.

The reason for the unusual SB behavior is now clear. The optimal active spaces that maximize the correlation energy for a given reference determinant differ for restricted and unrestricted wave functions. To a large extent, the correlation energy can be maximized without altering the reference energy at all. For example, mixing between active and inactive virtual orbitals to increase the active virtual space density on the carbon atom at the expense of the hydrogen does not change the occupied

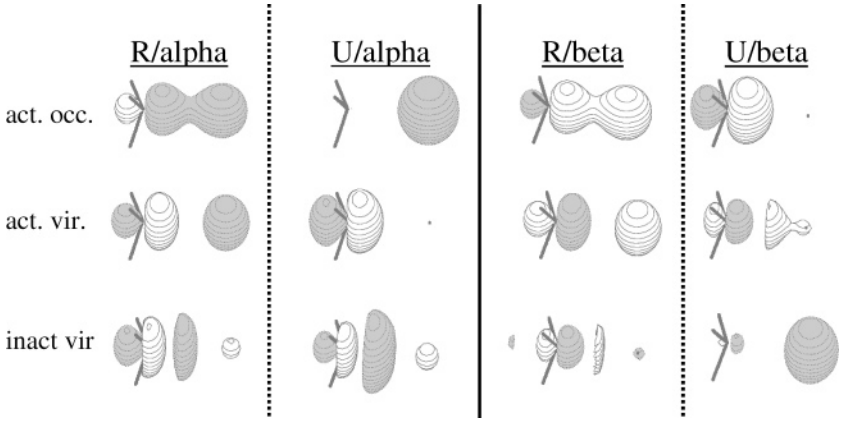

Figure 5. Corresponding orbitals between the restricted and unrestricted wave functions with the smallest overlap in each subspace at $R_{CH} = 2.450$ Å.

TABLE 3: Size-Consistency Error = $E_{supersystem} - E_{fragments}$ of UVOD/6-31G* at Dissociation

species	energy (E_h)
$^2CH_3$	−39.608129
^2H	−0.498233
$^1CH_3-H^a$	−40.116217
Error	−0.009854

[a] CH_3-H super system was computed with a 50 Å separation between the fragments.

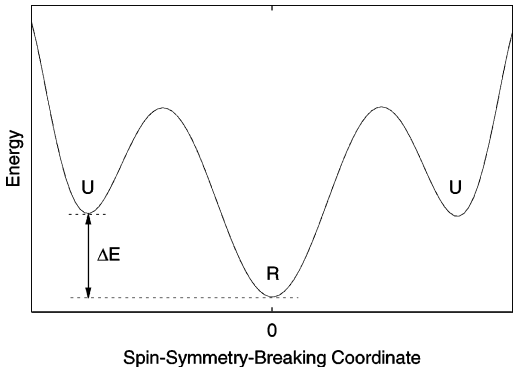

Figure 6. Schematic of an orbital rotation energy surface with respect to breaking spin symmetry in the orbitals for variationally optimized active space methods. $\Delta E = E_{unrest} - E_{rest}$. *R* and *U* label the restricted and unrestricted solutions, respectively.

virtual partitioning, so the reference energy remains the same, but it does allow the unrestricted wave function to capture more correlation energy. The restricted wave function, being delocalized over the whole molecule, prefers the original antibonding orbitals in the active virtual space.

These different optimal active spaces create different wave functions, and we arrive at a different view for the spin SB problem; one that is schematically shown in Figure 6. Before and after the crossover point, the restricted and unrestricted solutions are separate minima in the orbital rotation space. At the crossover point, the loss of correlation energy perfectly offsets the benefit of breaking spin symmetry in the reference, and $\Delta E = E_{unrest} - E_{rest} = 0$. At shorter bond distances, $\Delta E > 0$ (favoring the restricted solution), and beyond the SB point, $\Delta E < 0$ (favoring the unrestricted one). Not until some distance after the SB point, when the unrestricted solution lies far enough below the restricted one to eliminate the barrier between them, does the restricted solution develop an instability that leads to the unrestricted solution. In general, because of the difference in the optimal active spaces, the UVOD (or related method) wave function will not coincide with the restricted one, at least in the regime where a separate UHF solution exists, in stark contrast to the HF or OD case. In turn, this SB behavior destroys the size consistency of VOD and PP.

To rectify these problems, we propose a new model for spin-unrestricted active space methods where the spatial partitioning between the active and inactive subspaces will be identical (restricted) for both sets of spin orbitals, but the active orbitals will be allowed to break spin symmetry *within* the active space. For example, in the case of VOD, the new unrestricted model would allow the partitioning between active occupied and active virtual orbitals to differ in the alpha and beta spin cases, while ensuring that the space spanned by the union of the two active subspaces is identical.

In PP, the alpha and beta orbitals will be able to break spin symmetry by mixing individually between correlated pairs only, not by mixing with inactive orbitals, ensuring that this unusual SB phenomenon and its associated problems do not occur. In fact, for a single dissociating pair with these additional constraints, PP will no longer break spin symmetry at all, as we have verified by trying to break symmetry from *R*1 in methane with all inactive orbitals frozen to prevent their mixing with the active orbitals. With that additional constraint, *R*1 becomes stable for all bond lengths. This result is unsurprising: PP solves the pair problem exactly, and it includes pair interactions only at the mean-field level. Therefore, there is no impetus to break symmetry. Furthermore, whereas solution *R*2 in our example above would still exist (though it would require a very poor initial guess to find it), solution *U*2 would not occur because it requires that the inactive space be allowed to break spin symmetry. Of course, in accordance with the variational procedure used to determine the PP energy, this proposed additional constraint effectively raises the asymptotic total energy by roughly 9 kcal/mol (the energy separation between *R*1 and *U*2 at 3.5 Å). On the other hand, one hopes that the restoration of size consistency means that this higher total energy will provide better chemical properties (the atomization energy, for example).

Conclusion

Unlike spin SB in most quantum chemical model chemistries, the variational active space methods exhibit nonsmooth restricted to unrestricted transitions. This occurs because the wave function and the energy depend on the partitioning between the active and inactive spaces in addition to the partitioning of the occupied and virtual spaces, and because the orbital optimization is unconstrained. When breaking symmetry, wave functions can

often lower their energies by expanding the active space on one fragment at the expense of another fragment, giving a different wave function than one would obtain by studying either fragment alone. The two solutions have different optimal active spaces, which leads to two distinct, stable solutions that cross at the SB point. This result implies that, as defined currently, these unrestricted methods are not size consistent. In this light, previously computed UVOD and UPP results ought to be re-evaluated.

Although these issues undermine unrestricted active space methods in their current form, they can be reformulated to circumvent the SB and size consistency problems. Clearly, a more limited spin-unrestricted model is necessary. The simplest possibility is to constrain the partitioning between the active and inactive subspaces to be the same for both alpha and beta spin sets, but to allow the partitioning between the occupied and virtual orbitals within the active space to differ between the alpha and beta spin sets. This model should eliminate the artifactual SB behavior observed here and restore size consistency, and it merits further study. Looking ahead, UPP shows promising behavior for efficiently treating challenging radicals.[14] It should prove particularly interesting to reconsider the behavior of UPP with the new model for cases such as F_2^+ and allyl, both of which exhibit substantial symmetry-breaking effects under the current formulation.

Acknowledgment. Funding for this study was provided by the Director, Office of Energy Research, Office of Basic Energy Sciences, Chemical Sciences Division, of the U.S. Department of Energy under Contract No DEAC03-76SF00098. We thank J. Subotnik, Y. Shao, and T. Dutoi for their helpful discussions on the subject.

References and Notes

(1) Pople, J. A.; Nesbet, R. K. *J. Chem. Phys.* **1954**, *22*, 571−572.
(2) Jensen, F. *Chem. Phys. Lett.* **1990**, *169*, 519−528.
(3) Barnes, L. A.; Lindh, R. *Chem. Phys. Lett.* **1994**, *223*, 207−214.
(4) Hrušák, J.; Iwata, S. *J. Chem. Phys.* **1996**, *106*, 4877−4887.
(5) Nobes, R. H.; Pople, J. A.; Radom, L.; Handy, N. C.; Knowles, P. J. *Chem. Phys. Lett.* **1987**, *138*, 481−485.
(6) Lepetit, M. B.; Pélissier, M.; Malrieu, J. P. *J. Chem. Phys.* **1988**, *89*, 998−1008.
(7) Gill, P. M. W.; Pople, J. A.; Radom, L.; Nobes, R. H. *J. Chem. Phys.* **1988**, *89*, 7307−7314.
(8) Szabo, A.; Ostlund, N. S. *Modern Quantum Chemistry: Introduction to Advanced Electronic Structure Theory*; Dover: Mineola, NY, 1996.
(9) Roos, B. O. *Adv. Chem. Phys.* **1987**, *69*, 399−345.
(10) Krylov, A. I.; Sherrill, C. D.; Byrd, E. F. C.; Head-Gordon, M. *J. Chem. Phys.* **1998**, *109*(24), 10669−10678.
(11) Ukrainskii, I. I. *Theor. Math. Phys.* **1977**, *32*, 816−822.
(12) Cullen, J. *Chem. Phys.* **1996**, *202*, 217−229.
(13) Van Voorhis, T.; Head-Gordon, M. *J. Chem. Phys.* **2002**, *117*, 9190−9201.
(14) Beran, G. J. O.; Austin, B.; Sodt, A.; Head-Gordon, M. *J. Phys. Chem. A* **2005**, *109*, 9183−9192.
(15) Sodt, A.; Beran, G. J. O.; Jung, Y.; Austin, B.; Head-Gordon, M. *J. Comput. Theor. Chem.* **2006**, *2*, 300−305.
(16) Purvis, G. D., III; Bartlett, R. J. *J. Chem. Phys.* **1982**, *76*, 1910−1918.
(17) Head-Gordon, M.; Voorhis, T. V.; Beran, G. J.; Dunietz, B. D. *Computational Science-ICCS 2003, Pt IV, Proceedings Lecture Notes in Computer Science* **2003**, *2660*, 96−102.
(18) Beran, G. J. O.; Head-Gordon, M. *Mol. Phys.* **2006**, *104*, 1191−1206.
(19) Beran, G. J. O.; Head-Gordon, M.; Gwaltney, S. R. *J. Chem. Phys.* **2006**, *124*, 114107.
(20) Andersson, K.; Malmqvist, P.-Å.; Roos, B. O.; Sadlej, A. J.; Wolinksi, K. *J. Phys. Chem.* **1990**, *94*, 5483−5488.
(21) Gwaltney, S. R.; Sherrill, C. D.; Head-Gordon, M.; Krylov, A. I. *J. Chem. Phys.* **2000**, *113*, 3548−3560.
(22) Krylov, A. I. *J. Chem. Phys.* **2000**, *113*, 6052−6062.
(23) Saebø, S.; Pulay, P. *Annu. Rev. Phys. Chem.* **1993**, *44*, 213−236; and references therein.
(24) Russ, N. J.; Crawford, T. D. *J. Chem. Phys.* **2004**, *121*, 691−696.
(25) Hehre, W. J.; Ditchfield, R.; Pople, J. A. *J. Chem. Phys.* **1972**, *56*, 2257−2261.
(26) Shao, Y.; Molnar, L. F.; Jung, Y.; Kussmann, J.; Ochsenfeld, C.; Brown, S. T.; Gilbert, A. T. B.; Slipchenko, L. V.; Levchenko, S. V.; O'Neill, D. P.; DiStasio, R. A., Jr.; Lochan, R. C.; Wang, T.; Beran, G. J. O.; Besley, N. A.; Herbert, J. M.; Lin, C. Y.; Van Voorhis, T.; Chien, S. H.; Sodt, A.; Steele, R. P.; Rassolov, V. A.; Maslen, P. E.; Korambath, P. P.; Adamson, R. D.; Austin, B.; Baker, J.; Byrd, E. F. C.; Dachsel, H.; Doerksen, R. J.; Dreuw, A.; Dunietz, B. D.; Dutoi, A. D.; Furlani, T. R.; Gwaltney, S. R.; Heyden, A.; Hirata, S.; Hsu, C.-P.; Kedziora, G.; Khalliulin, R. Z.; Klunzinger, P.; Lee, A. M.; Lee, M. S.; Liang, W.; Lotan, I.; Nair, N.; Peters, B.; Proynov, E. I.; Pieniazek, P. A.; Rhee, Y. M.; Ritchie, J.; Rosta, E.; Sherrill, C. D.; Simmonett, A. C.; Subotnik, J. E.; Woodcock, H. L., III; Zhang, W.; Bell, A. T.; Chakraborty, A. K.; Chipman, D. M.; Keil, F. J.; Warshel, A.; Hehre, W. J.; Schaefer, H. F., III; Kong, J.; Krylov, A. I.; Gill, P. M. W.; Head-Gordon, M. *Phys. Chem. Chem. Phys.* **2006**, *8*, 3172−3191.
(27) Sherrill, C. D.; Krylov, A. I.; Byrd, E. F. C.; Head-Gordon, M. *J. Chem. Phys.* **1998**, *109*(11), 4171−4181.
(28) Woon, D. E.; Dunning, T. H., Jr. *J. Chem. Phys.* **1995**, *103*, 4572−4585.
(29) Weigend, F.; Köhn, A.; Hättig, C. *J. Chem. Phys.* **2002**, *116*, 3175−3183.
(30) King, H. F.; Stanton, R. E.; Kim, H.; Wyatt, R. E.; Parr, R. G. *J. Chem. Phys.* **1967**, *47*, 1936−1941.
(31) Schaftenaar, G.; Noordik, J. H. *J. Comput.-Aided Mol Design* **2000**, *14*, 123−134.